

Dynamic Behavior and Stability of a Disk Brake Coupled with a Helical Geared System

Ahmed Ghorbel*, Bacem Zghal**, Moez Abdennadher**, Lassaad Walha**, Mohamed Haddar**

Keywords : Disk brake, helical gear, stability, dynamic behavior

ABSTRACT

The application of friction mechanisms is found in many areas such as automobile disc brakes. The study of these systems presents some complexity due to the large number of components and parameters included. In this paper a mathematical mechanical modeling of disc brake squeal with multi friction contacts points is developed. Besides, an analysis of squeal is presented through the study of stability of the equilibrium by calculating the complex Eigen modes. Then, the influence of angular velocity of the disc, phase shift angle between two contacts points in the same side of disc, coefficient of friction and the linear stiffness and damping is investigated. In the second part of this paper, the disc brake model will be coupled with a helical geared system. This mechanical model has eight degrees of freedom. The dynamic response of the non-linear system is computed using Runge Kutta method. Dynamic responses come to confirm a significant influence of disc brake on the dynamic behavior of gear.

INTRODUCTION

Whatever the scope, the friction mechanisms coupled with gearbox have an important dynamic wealth, due to the number of components that constitute them, and a proven mechanical complexity. Reducing vibrations of a coupled system requires a better understanding of the behavior of any subsystem.

Paper Received May 2016. Revised July, 2017. Accepted August, 2017. Author for Correspondence: Ahmed Ghorbel.

** Associate Professor, Mechanical, Modeling and Manufacturing Laboratory LA2MP, National School of Engineers of Sfax, TUNISIA, BP 1173-3038 Sfax, Tunisia.

* Engineer and Phd in mechanical engineering, Mechanical, Modeling and Manufacturing Laboratory LA2MP, National School of Engineers of Sfax, TUNISIA, BP 1173-3038 Sfax, Tunisia.

The disc brake system has a certain mechanical complexity including many parts resulting in point or surface contact and friction. This can be a good reason for generating noise. An experimental test shows that the brake noise is most often the result of self-excited vibrations arising from friction contact between the pad and the disc. The squeal is the best known example.

However, many researchers and design engineers worldwide have studied squeal generation mechanisms but so far there is not a full explanation by the complexity of the problem. Wagner et al. (2007), Oberst and Lai (2011), Kinkaid et al. (2002) and Shin et al. (2002) give a great insight into the modeling of disc brake squeal phenomenon. An analytical model of the wobbling dynamics of friction disks and an investigation about the limit cycle of the wobbling disc is studied by Alexendar et al. (2011). The observations Fosberry and Holubecki (1961) showed that the vibrations of the disc are much larger than those of the caliper of about 20 μm . It has a dominant role in the modeling of squeal, hence the importance of studying the vibration effect disk especially when it is coupled by another system as a gearbox. To reduce brake squeal, it is possible to increase the rigidity of the disc, use a viscoelastic material for trim or change the form of brake pads (Liu et al., 2007). Generally, the rotor of a disc brake is driven in rotation by a gear mechanism. In this context, M.T. Khabou et al. (2014) studied the influence of the friction phenomenon generated by a disc brake on the dynamic behavior of a single gear stage. This investigation is not sufficient to determine the influence of brake parameters on the dynamic behavior of the system since it uses a simple brake model.

To determine the vibration in helical gears, a dynamic model was developed by Andersson and Vedmar (2003). Furthermore, Walha et al. (2009) treated a model of helical gear system with two floors. Therefore, it is necessary to develop a model with which the effect of helical geared system in dynamic behavior of the disc brake can be analysed.

The main goal of this paper is to develop an analytical mathematical modeling of brake squeal with four contact points. The influence of kinematic and physical parameters on the analyses of Lyapunov stability of the braking system will be investigated.

After that, the model of disc brake is coupled with helical gear reducer is presented and the objective of this study is to determine the influence of disk brake on the dynamic behavior of the coupled system.

DYNAMIC MODEL OF A DISC BRAKE COUPLED WITH HELICAL GEARED SYSTEM

Fig. 1 shows the model of the studied system, it consists of two main blocks: The first presents the gearbox with helical gear and the second characterizes the model of disc brake with multi friction contacts. This system has eight degrees of freedom of rotation.

The gear is composed of a motor whose moment of inertia is I_M , a flexible bearing, a gear base radius R_p whose moment of inertia I_p , and a wheel whose base radius is R_r with a moment of inertia I_r . The second block is the disc brake model that will be detailed in the section 3.1. The two shafts are modeled by torsional

stiffness K_{si} and dampers C_{si} and the two blocks are supported by flexible bearing with K_{yi} and C_{yi} which present respectively the traction-compression stiffness and damping.

θ_M, θ_p and θ_R are respectively the angular displacement of the motor, the pinion and the toothed wheel. q_1, q_2 and q_3 are the angular rotation of brake disc. The vertical displacements of the two shafts of transmission are defined by y_1 and y_2 .

Dynamic model of a disc brake coupled with a single-stage gearbox is described in this section. The motion transmission mechanism is made by helical geared system. The gears are treated as rigid cylinders linked by a meshing stiffness that is, relatively accurate, the contributions of all the deformable parts (deformed contact, teeth bending ...). The torsional models rely on traditional springs and concentrated masses approaches types. The gears have only one degree of freedom of twist and are linked together by gear mesh stiffness.

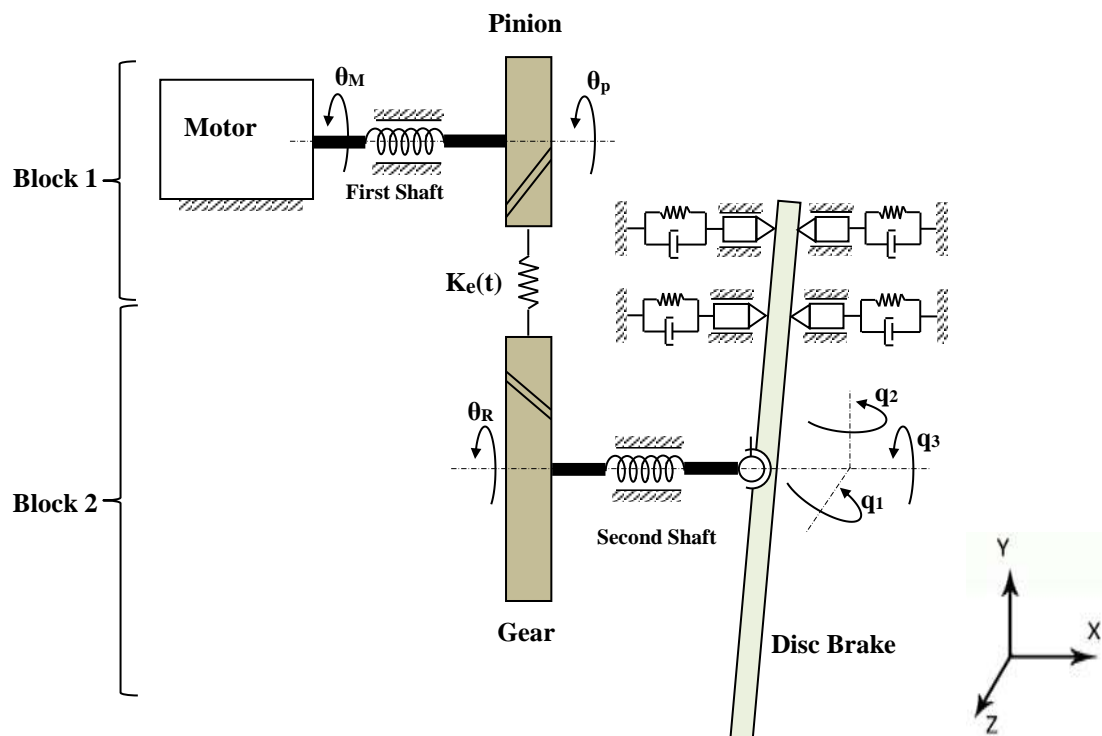


Fig. 1. Model of a disc brake with gearbox

MATHEMATICAL DEVELOPMENT OF DISC BRAKE MODEL

General description of the disc brake model

Despite the large number of studies concerned with modeling automotive disc brakes in the literature, there is a lack of an analytical model which takes into account the geometry of the brake pad and the location of the contact forces. A literature review of analytical

models for disc brake modeling proves that researchers are working with a single point of frictional contact for every face of the disc.

Therefore, a new minimal model with two degrees of freedom is introduced to analyze the influence of positional variation between two contact points in the same face of the disc, taking into account the vibration of the disc as it plays an important role in the squeal.

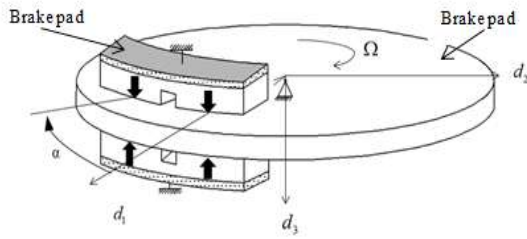


Fig. 2. Disc brake model

In order to study the phenomenon of disc brakes squeal, a model with two degrees of freedom has been published in (Wagner et al., 2007) that represents a rigid oscillating disc in frictional contact with two plates. Spelsberg-Korspeter et al. (2009), takes disc of the brake as a Kirchhoff plates. Based on the publications (Wagner et al., 2007; Hochlenert et al.,

2007; Spelsberg-Korspeter et al., 2009), the author in (Hochlenert et al., 2010) modeled the disc as a rigid disc of thickness h . The assumption of a constant speed of the disc is presented in all these investigations.

In order to improve disc brakes models, a new minimum model with two degrees of freedom is shown in Fig 2. This model has a rigid wobbling disc (thickness h , rotational stiffness k_r , rotational damping coefficient d_r and the inertia tensor I_D) and brake pads which are modeled by the four mass into frictional contact with the disc (friction coefficient μ). A coordinate system d_1, d_2 and d_3 is fixed to the disc which oscillates relative to another coordinate system n_1, n_2 and n_3 , and the orientation of the disc is described by three cardan angles q_i ($i = 1, 2, 3$) and two intermediate coordinate systems a_i and b_i ($i = 1, 2, 3$). See Fig. 3 and Fig. 4.

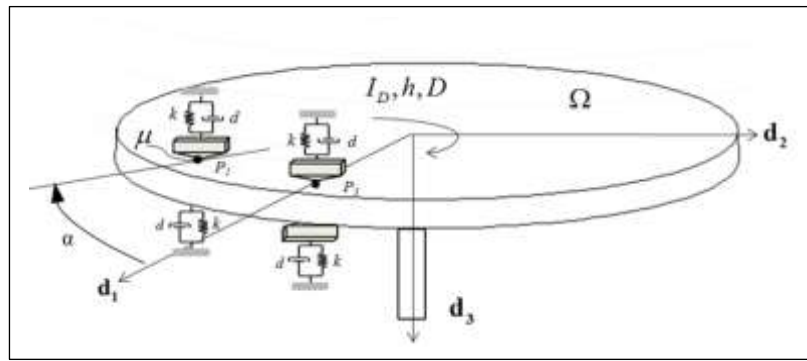


Fig. 3. New disk brake model

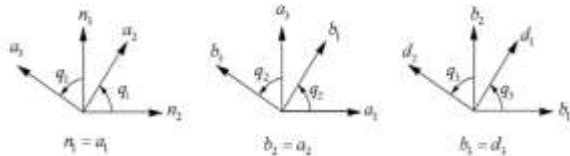


Fig. 4. Coordinate systems

The resulting angular velocity of the disc is given by the following equation:

$$\omega_{N \rightarrow D} = \dot{q}_1 \mathbf{n}_1 + \dot{q}_2 \mathbf{a}_2 + \dot{q}_3 \mathbf{d}_3 \quad (1)$$

In the first part, we take a constant angular velocity along \mathbf{n}_3

$$\omega_{\mathbf{n}_3} = (\Omega + \dot{q}_3) \mathbf{n}_3 \quad (2)$$

Kinematic analysis

Determination of the contact points

Since platelets are fixed with respect to the base ($\mathbf{n}_1, \mathbf{n}_2, \mathbf{n}_3$), the vectors of contact points coordinates presented in Fig. 3 can be written in the next form:

$$\mathbf{P}_1 = -r \mathbf{n}_2 + (h_1 - \frac{h}{2}) \mathbf{n}_3 \quad (3)$$

$$\mathbf{P}_2 = -r \mathbf{n}_2 + (h_2 - \frac{h}{2}) \mathbf{n}_3 \quad (4)$$

$$\mathbf{P}_3 = r(-\cos(\alpha) \mathbf{n}_2 + \sin(\alpha) \mathbf{n}_1) + (h_3 - \frac{h}{2}) \mathbf{n}_3 \quad (5)$$

$$\mathbf{P}_4 = r(-\cos(\alpha) \mathbf{n}_2 + \sin(\alpha) \mathbf{n}_1) + (h_4 - \frac{h}{2}) \mathbf{n}_3 \quad (6)$$

Every disk brake pad is modeled by two masses in a same face dephased an angle α relative to each other with the same radius r relative to the disc center, and each mass is supported by a spring k and damper d which are preloaded with preload N_0 .

On the other side, to have contact between the disc and the pads, it is necessary that the vectors of the positions of contact points for the pads and the rotor are equal. After linearization for small angles, the displacement vectors in the base ($\mathbf{b}_1, \mathbf{b}_2, \mathbf{b}_3$) can be expressed

$$\mathbf{P}_1 = \frac{h}{2} q_2 \mathbf{b}_1 + (-r + \frac{h}{2} q_1) \mathbf{b}_2 - \frac{h}{2} \mathbf{b}_3 \quad (7)$$

$$\mathbf{P}_2 = -\frac{h}{2} q_2 \mathbf{b}_1 + (-r - \frac{h}{2} q_1) \mathbf{b}_2 + \frac{h}{2} \mathbf{b}_3 \quad (8)$$

$$\mathbf{P}_3 = (\frac{h}{2} q_2 + r \sin(\alpha)) \mathbf{b}_1 + (-r \cos(\alpha) + \frac{h}{2} q_1) \mathbf{b}_2 - \frac{h}{2} \mathbf{b}_3 \quad (9)$$

$$\mathbf{P}_4 = (-\frac{h}{2} q_2 + r \sin(\alpha)) \mathbf{b}_1 + (-r \cos(\alpha) - \frac{h}{2} q_1) \mathbf{b}_2 + \frac{h}{2} \mathbf{b}_3 \quad (10)$$

where h_1, h_2, h_3 and h_4 represents the corresponding movements of the pads with respect to the static

equilibrium, and therefore the displacement of the springs.

$$h_1 = h_2 = -r \cdot q_1 \quad (11)$$

$$h_3 = h_4 = -r \cdot \cos(\alpha) \cdot q_1 - r \cdot \sin(\alpha) \cdot q_2 \quad (12)$$

The direction of the frictional force is given by the vector of relative speed between the two bodies in contact.

$$\mathbf{r}_i = \frac{v_i - v'_i}{|v_i - v'_i|} \text{ with } i = 1, 2, 3 \text{ and } 4 \quad (13)$$

where v_i and v'_i are respectively the velocity of the material points on the surface of the disc in contact with the pad and the velocity of the contact points of the pads.

Determination of the contacts forces

In this section, the contacts forces acting between the disc and the pads are studied.

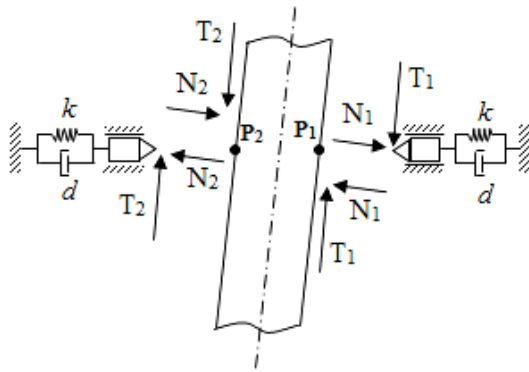


Fig. 5. Schematic representation for the contact forces

The tangential frictional forces are proportional with the normal forces by the friction coefficient μ depending on the nature of the materials and surface condition of the two bodies in contact (Fig. 5). Concerning the contact law in the literature (Ouyang et al., 2000; Tuchinda et al., 2001; Tuchinda et al., 2002; Denou et al., 2001), many authors use a constant friction coefficient and the assumption of no stick-slip behavior. The effect of stick-slip between the disc and the brake pads can be neglected because the relative speed at the macroscopic level may disappear during squeal, this estimate is verified experimentally by Hochlenert et al. (2014), So, Coulomb friction model is chosen as a model of which is largely sufficient to model the disc brake squeal.

$$\begin{aligned} T_1 &= \mu \cdot N_1 \\ T_2 &= \mu \cdot N_2 \\ T_3 &= \mu \cdot N_3 \\ T_4 &= \mu \cdot N_4 \end{aligned} \quad (14)$$

The resulting contact forces on the disc is written in the following form

$$\begin{aligned} \mathbf{F}_1 &= -T_1 \cdot \mathbf{r}_1 + N_1 \cdot \mathbf{d}_3 \\ \mathbf{F}_2 &= -T_2 \cdot \mathbf{r}_2 - N_2 \cdot \mathbf{d}_3 \\ \mathbf{F}_3 &= -T_3 \cdot \mathbf{r}_3 + N_3 \cdot \mathbf{d}_3 \\ \mathbf{F}_4 &= -T_4 \cdot \mathbf{r}_4 - N_4 \cdot \mathbf{d}_3 \end{aligned} \quad (15)$$

Break disc is presented as a rotating Kirchhoff plate with constant speed of rotation Ω . In this mathematical modeling, the fluctuation of angular velocity in the input of the disc brake is neglected. Therefore, it can be written as follows:

$$\omega \cdot \mathbf{n}_3 = \Omega, \text{ and } \dot{q}_3 = \ddot{q}_3 = 0 \quad (16)$$

In the formalism of analytical mechanics, the theorem of kinetic moment for a material point is used. Hence the angular momentum

$$\frac{d}{dt} I_D \cdot \omega = M \quad (17)$$

where

$$\mathbf{I}_D = \begin{bmatrix} I_{D1} & 0 & 0 \\ 0 & I_{D2} & 0 \\ 0 & 0 & I_{D3} \end{bmatrix}_d \quad (18)$$

$$\omega = [\omega_1 \ \omega_2 \ \omega_3]_d \quad (19)$$

$$\mathbf{M} = [M_1 \ M_2 \ M_3]_d \quad (20)$$

Governing equations of motion

The motion equations resulting balance of angular momentum of the disc and the moments of the external forces acting can be expressed in equation (21).

$$\begin{cases} I_{D1} \ddot{q}_1 + \Omega I_{D3} \dot{q}_2 = M_1 \\ I_{D2} \ddot{q}_2 - \Omega I_{D3} \dot{q}_1 = M_2 \\ I_{D3} \ddot{q}_3 = M_3 = 0 \end{cases} \quad (21)$$

The resisting torque on the disc M (see equation 22) is given by the sum of the torque of the contact forces from the center of the disc, the torque due to the viscoelastic suspension and M_A torque constraint.

$$\mathbf{M} = -(k_t \cdot q_1 + d_t \cdot \dot{q}_1) \cdot \mathbf{n}_1 - (k_t \cdot q_2 + d_t \cdot \dot{q}_2) \cdot \mathbf{b}_2 + \mathbf{P}_1 \wedge \mathbf{F}_1 + \mathbf{P}_2 \wedge \mathbf{F}_2 + \mathbf{P}_3 \wedge \mathbf{F}_3 + \mathbf{P}_4 \wedge \mathbf{F}_4 + M_A \cdot \mathbf{n}_3 \quad (22)$$

Where

$$\mathbf{P}_1 \wedge \mathbf{F}_1 = N_1 \cdot \begin{pmatrix} -r + \frac{h}{2} q_1 + \frac{\mu h^2}{4r} \left(\frac{\dot{q}_1}{\Omega} + q_2 \right) \\ -\frac{\mu h}{2} - \frac{h}{2} q_2 \\ \mu r - \frac{\mu h}{2} q_1 \end{pmatrix}_D \quad (23)$$

$$\mathbf{P}_2 \wedge \mathbf{F}_2 = N_2 \cdot \begin{pmatrix} r + \frac{h}{2}q_1 + \frac{\mu h^2}{4r}(\dot{q}_1 + q_2) \\ \frac{\mu h}{2} - \frac{h}{2}q_2 \\ \mu r + \frac{\mu h}{2}q_1 \end{pmatrix}_{\mathbf{D}} \quad (24)$$

$$\mathbf{P}_3 \wedge \mathbf{F}_3 = N_3 \cdot \begin{pmatrix} r \cdot \cos(\alpha) + \frac{h}{2}q_1 + \frac{\mu h^2}{4r}(\dot{q}_1 + q_2) \\ -\frac{\mu h}{2} - \frac{h}{2}q_2 - r \cdot \sin(\alpha) \\ \mu \cdot r \cdot \cos(\alpha) + \frac{\mu h}{2}(\dot{q}_1 + q_2) \sin(\alpha) - \frac{\mu h}{2}q_1 \end{pmatrix}_{\mathbf{D}} \quad (25)$$

$$\mathbf{P}_4 \wedge \mathbf{F}_4 = N_4 \cdot \begin{pmatrix} r \cdot \cos(\alpha) + \frac{h}{2}q_1 + \frac{\mu h^2}{4r}(\dot{q}_1 + q_2) \\ \frac{\mu h}{2} - \frac{h}{2}q_2 + r \cdot \sin(\alpha) \\ \mu \cdot r \cdot \cos(\alpha) + \frac{\mu h}{2}(\dot{q}_1 + q_2) \sin(\alpha) + \frac{\mu h}{2}q_1 \end{pmatrix}_{\mathbf{D}} \quad (26)$$

The forces applied by each contact point of the disc surface are equal because it undergoes the same pressure as the piston and have the same rigidity (same pad). The dynamic forces of friction obtained are complex in nature. This complexity is due to the large number of influencing factors.

$$\begin{aligned} N_1 = N_3 &= k \cdot r \cdot q_1 + d \cdot r \cdot \dot{q}_1 - N_0 - \mu \cdot N_0 \cdot q_2 \\ N_2 = N_4 &= -k \cdot r \cdot q_1 - d \cdot r \cdot \dot{q}_1 + N_0 + \mu \cdot N_0 \cdot q_2 \end{aligned} \quad (27)$$

Using equations from (1) to (27), the governing motion equation in matrix form for a model of the disk brake is obtained in following form (Eq. 28):

$$\begin{bmatrix} I_{D1} & 0 \\ 0 & I_{D2} \end{bmatrix} \begin{bmatrix} \ddot{q}_1 \\ \ddot{q}_2 \end{bmatrix} + \begin{bmatrix} \frac{\mu h^2 N_0}{2r\Omega} + d_t + 2dr^2(1 + \cos(\alpha)) \\ -\Omega I_{D3} - 2d(\mu r h + r^2 \sin(\alpha)) \end{bmatrix} \begin{bmatrix} \dot{q}_1 \\ \dot{q}_2 \end{bmatrix} + \begin{bmatrix} \frac{\mu h^2 N_0}{2r} \\ k_t + 2N_0(h + \mu^2 h + r\mu \sin(\alpha)) \end{bmatrix} \begin{bmatrix} q_1 \\ q_2 \end{bmatrix} = \begin{bmatrix} 0 \\ 0 \end{bmatrix} \quad (28)$$

STABILITY ANALYSIS OF DISC BRAKE MODEL

The purpose is to find a contribution between the system's speed and brake settings is presented in Fig. 3, to work in the stable area to study the dynamic behavior of the global system in Fig. 1.

The numerical study of the stability leads to solve a problem for generalized eigenvalues, and among the aims of this work is to assess the sensitivity of the eigenvalues relative to the geometry of the brake pad. Another aim is to avoid the destabilization of a chosen way by finding an approach between the rotation speed of the disk and the orientation angle of contact points.

Good dynamic and stability study requires careful selection of the disc brake parameters. The parameters chosen in this work corresponds to the result of detailed experimental studies on a test bench at the TU Darmstadt, and these results have been presented in several models for modeling of the disc brake. U von Wagner et al. (2007), identified these parameters to investigate the stability of a disc brake squeal model. Also, the authors in Ref (Wagner et al., 2004) used a model with four degrees of freedom to eliminate the squeal with the parameters in Table 1. On

the other work (Jearsiripongkul, 2005), author has taken for their model with two degrees of freedom. Some parameters are varied to mount their effect on system stability.

The stability of solution is studied on the basis of the linearized equation of motion, i.e. the indirect method of Lyapunov. Replacing $q(t) = \tilde{q}e^{\lambda t}$ in the equation of motion, where an unstable solution corresponds to a positive real part of λ . The two essential parameters to be investigated are the angular velocity Ω and the phase shift angle α .

For the new disc brake model developed in this paper, the Fig. 6-a represents the location of the eigenvalues to a variable rotation speed and a phase shift between two contact points. This figure shows the eigenvalues of positive real part, so the solution becomes unstable and self-excited vibrations are interpreted, hence squeal is the cause of the low brake pressure and high disk rotation speed. The number of unstable poles increases to increasing the phase shift α . We can verify these results by comparing them with the model proposed by von Wagner et al. (2007). Fig. 6-b shows root locus of the eigenvalues for a simple model with only two contact points.

The critical speed is the speed at the limit of

stability, for values to real part near zero. Manufacturers of disc brakes will cause some changes to solve the instability problems. Therefore, others parameters can be investigated in this section, such as stiffness k , damping of the pad d , rotational damping of the disc d_i and friction coefficient μ .

Fig. 7 indicates the variation of the critical speed Ω_{crit} to vary the stiffness k to four phase shift values α . The dependence of the critical speed of the stiffness value is drawing a line. In that which follows, this line characterizes linear stability boundary of the system

and it can be considered as the speed of rotation limit of the brake shaft above which Eigenvalues positive real part occurs and below which all the eigenvalues of the linearized system. It may be noted that the critical speed increases for low rigidity plate and the zone of stability increases to a low phase shift between the points of contact.

Table 1. Nominal values of disc brake parameters

Parameter	Symbol	Value
Distance of the pads from the center of the disk	r	0.13 m
Thickness of disk	h	0.02 m
Moment of inertia, with respect to d_1 and d_2	I_{D1}, I_{D2}	0.16 kg/m ²
Moment of inertia, with respect to d_3	I_{D3}	0.32 kg/m ²
Rotational stiffness	k_t	1.88 e ⁷ Nm
Rotational dampers	d_i	0.1 N m s
Nominal contact stiffness	k	6 e ⁶ N m
Nominal contact dampers	d	5 Ns /m
Preload	N_0	3000 N
friction coefficient	μ	0.3
Angle between two contact points	α	$[\pi/6 \ \pi/2]$

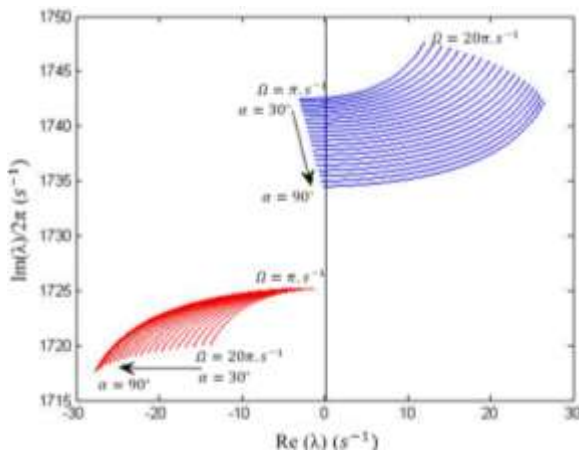


Fig.6-a. Root locus of the eigenvalues for varying Ω for each α (Upper half-plane shown only)

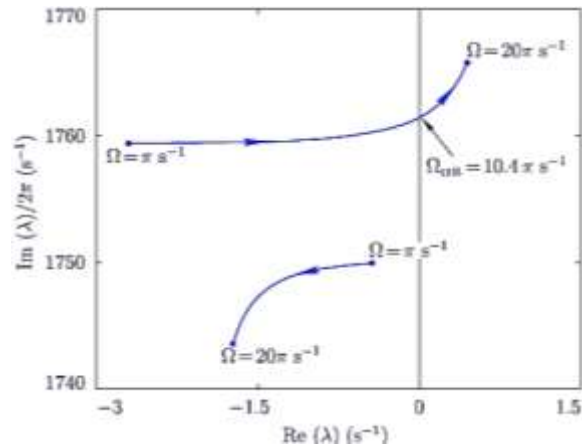


Fig.6-b. Root locus of the eigenvalues for varying Ω (Upper half-plane shown only) (Wagner et al., 2007)

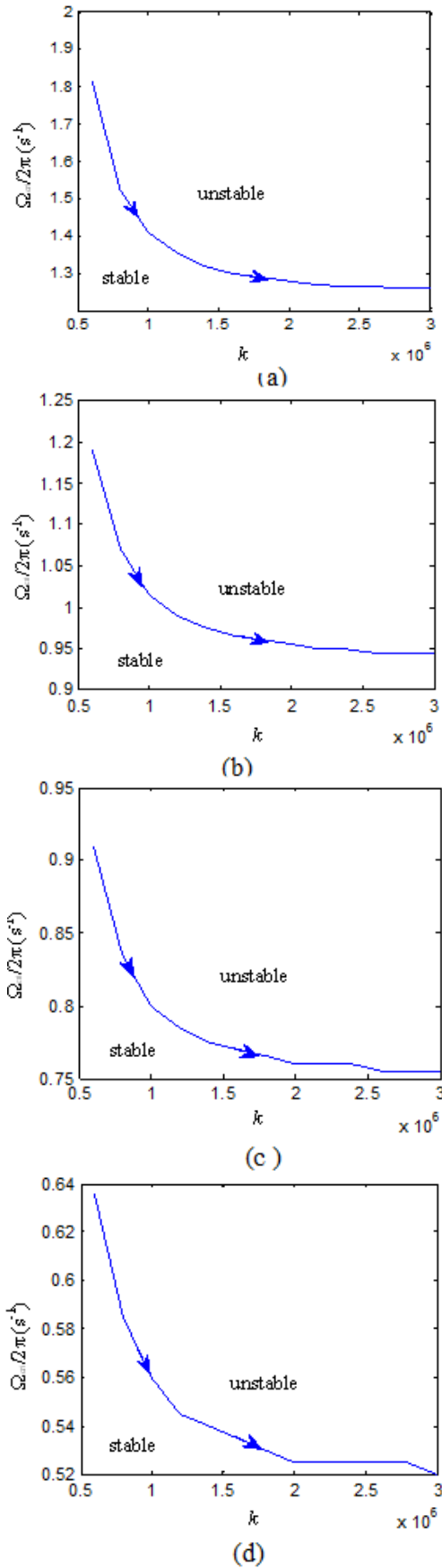


Fig. 7. Critical speed for varying k (a) $\alpha = \pi/6$, (b) $\alpha = \pi/4$, (c) $\alpha = \pi/3$ and (d) $\alpha = \pi/2$.

Other significant parameters can affect system stability zone are the damping of brake pads. Fig. 8 presents the critical speed for the variable damping pad d for four angles α and it may be concluded that increasing damping and low offset angle seems to stabilize friction-induced vibrations. The dependence of the critical speed on the damping coefficient d_t is presented in Fig. 9 and that indicates an increase of rotation damping and phase shift α always has a stabilizing characteristic. These results are confirmed by the research work in reference (Hagedom et al., 2014). In these two parametric studies, it has been concluded that increasing damping of the system, and phase shift angle have a worse effect and cannot be considered as an effective solution to avoid instability for the brake system.

Choosing a static friction model is the Coulomb model is largely sufficient to model the instability of self-existed of a disc brake vibrations but the value of this coefficient can affect system stability Fig.10 shows the critical speed variation as a function of friction coefficient, and it demonstrates the sensibility of a brake system friction coefficient and the position of the contact points.

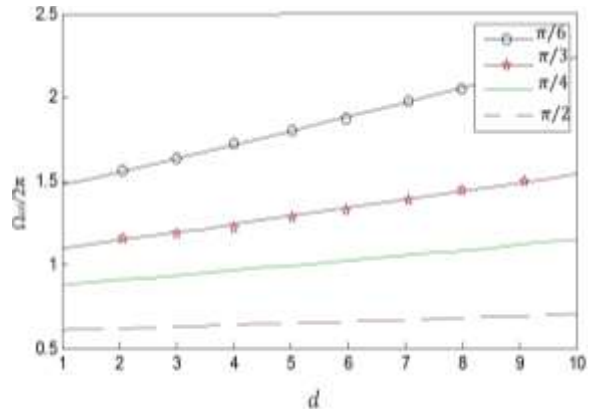


Fig.8. Critical speed for varying d

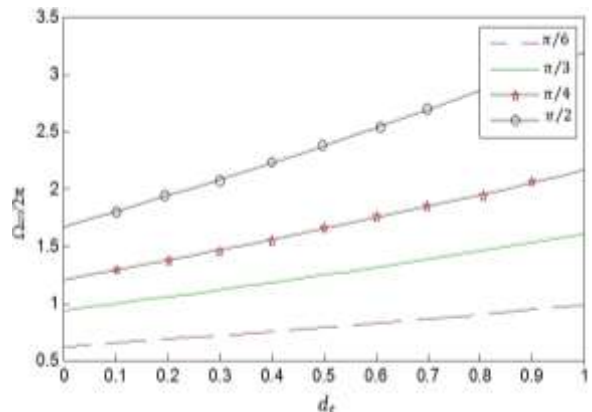


Fig.9. Critical speed for varying d_t

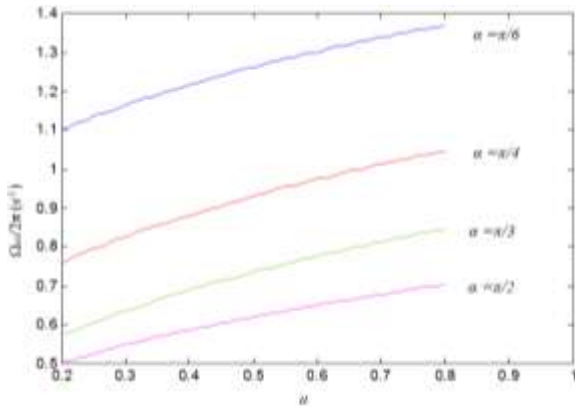


Fig.10. Critical speed for varying μ

Fig. 11 confirms that to increase the zone of stability, it is necessary that the phase shift angle α should be as low as possible but when the value α is lower, braking performance declines taking the example of the disc brake of a train or TGV. The squeal phenomenon can be more important, although this type of brake with a large number of contact points performs well. Hence manufacturers of automobile disc brakes must find a contribution between the acoustic phenomenon due to the self-vibration existed, and braking performance.

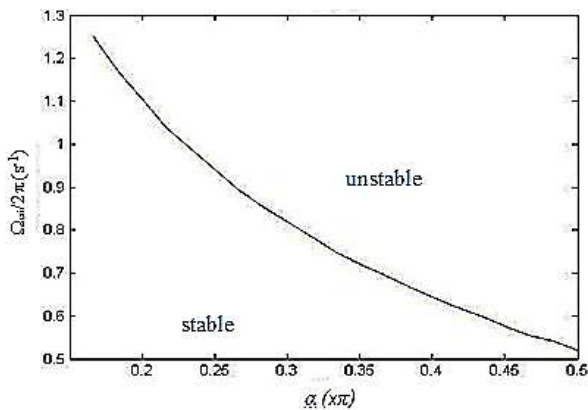


Fig.11. Critical speed for varying α

All the results demonstrate that the zone of stability depends on the selected physical and geometrical parameters and the correct choice of these parameters allows us to reduce the appearance of self-vibrations existed.

GLOBAL DYNAMIC BEHAVIOR OF A DISC BRAKE COUPLED WITH HELICAL GEARED SYSTEM

As a next step, the disc brake is coupled with a single helical gear stage. The powertrain system makes vibrations along y due to the flexible bearing. This oscillation is transmitted to the brake disc (Fig. 12). A guiding system used to constrain the oscillations of the disc in the horizontal plane and in the perpendicular direction to the axis of the stiffness k and damping d . The mathematical modeling of this relation is expressed as follows:

The pads have the same spring constant k , the same initial length l_0 and the guide system causes the same elongation Δl . Hooke's law gives:

$$F_1 \cdot \vec{y} = F_2 \cdot \vec{y} = -k \cdot \Delta l \cdot \sin(\alpha) \cdot \vec{y} \quad (29)$$

$$\Delta l = l - l_0 \quad \text{with}$$

$$l = \sqrt{z^2 + y_2^2} \quad \text{and} \quad \sin(\alpha) = \frac{y_2}{l} \quad (30)$$

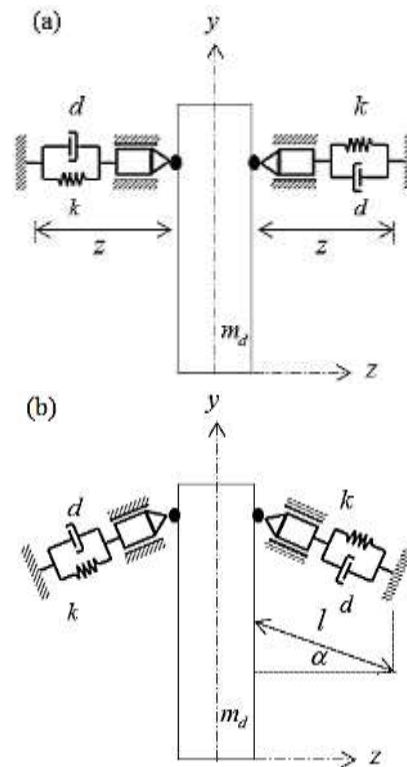


Fig.12. Diagram of the device in the plane (y, z) :
(a) $t=0$, (b) $t > 0$

A small oscillation $y_2 \ll z$, we can write $\frac{y_2}{z} \ll 1$.

Applying development limited to the first order to simplify the equation of the forces due to the linear stiffness k .

$$F_i = -k \cdot \Delta l \cdot \sin(\alpha) = -k \cdot y_2 \cdot \left(1 - \frac{l_0}{z}\right) \quad (31)$$

$$F_i = -cst \cdot k \cdot y_2 \quad \text{with } i=1,2,3 \text{ and } 4.$$

The Kinetic moment theorem is used to develop the mathematical model of the brake and Lagrange's method is used to formulate the differential equation governing of the gearbox system. The fluctuation of rotation speed of the disc brake should be taken into account in this section. It has to note the linearized system of disc brake and the helical gear transmission is coupled in angular velocity q_3 . The global nonlinear motion equations of the two blocks assembly (brake system block and the gearbox block) give the following array writing:

Table 2. The coefficients of $K(t)$

Notation	Analytic expression
s_1	$\cos \beta . \cos \alpha_1$
s_2	$R_p \cos \beta$
s_3	$R_r \cos \beta$

$$\left\{ \begin{array}{l}
 * m_{b1} \ddot{y}_1 + C_{y1} \dot{y}_1 + k_{y1} y_1 + s_1 k_1(t) \delta(t) = 0 \\
 * m_{b2} \ddot{y}_2 + C_{y2} \dot{y}_2 + 4.c.cst. \dot{y}_2 + k_{y2} y_2 + 4.k.cst. y_2 - s_1 k_1(t) \delta(t) = 0 \\
 * I_m \ddot{\theta}_m + C_{sh1} (\dot{\theta}_m - \dot{\theta}_p) + C_{p1} \dot{\theta}_m + k_{sh1} (\theta_m - \theta_p) = 0 \\
 * I_p \ddot{\theta}_p - C_{sh1} (\dot{\theta}_m - \dot{\theta}_p) + C_{p1} \dot{\theta}_p - k_{sh1} (\theta_m - \theta_p) + s_2 k_1(t) \delta(t) = 0 \\
 * I_r \ddot{\theta}_r + C_{sh2} (\dot{\theta}_r - \dot{q}_3) + C_{p2} \dot{\theta}_r + k_{sh2} (\theta_r - q_3) + s_3 k_1(t) \delta(t) = 0 \\
 * I_{d1} \ddot{q}_1 + (d_r + 2dr^2(1 + \cos(\alpha))) \dot{q}_1 + (2hN_0 + k_r + 2kr^2(1 + \cos(\alpha))) q_1 + \\
 \frac{\mu h^2 N_0}{2r} q_2 + \frac{\mu h^2 N_0}{2r(\Omega + q_3)} \dot{q}_1 - I_{d3} (\Omega + \dot{q}_3) \dot{q}_2 = 0 \\
 * I_{d2} \ddot{q}_2 + d_r \dot{q}_2 + (-2dr(\mu h + r.\sin(\alpha))) \dot{q}_1 + (k_r + 2N_0(h + h\mu^2 + r\mu.\sin(\alpha))) q_2 + \\
 (-2\mu r N_0(1 + \cos(\alpha)) - 2kr(\mu h + r.\sin(\alpha))) q_1 - I_{d3} (\Omega + \dot{q}_3) \dot{q}_1 = 0 \\
 * I_{d3} \ddot{q}_3 + C_{sh2} (\dot{q}_3 - \dot{\theta}_r) + C_{p2} \dot{q}_3 + k_{sh2} (q_3 - \theta_r) = 0
 \end{array} \right. \quad (32)$$

where the terms s_i are the coefficients of $K(t)$ given in table 2

The general differential motion equation of the system in matrix form can be expressed by:

$$[M] \left\{ \ddot{q} \right\} + [C] \left\{ \dot{q} \right\} + [K(t)] \{q\} = 0 \quad (33)$$

where $\{q\}$ is the vector of degrees of freedom:

$$[C] = \begin{bmatrix}
 C_{y1} & 0 & 0 & 0 & 0 & 0 & 0 & 0 & 0 \\
 0 & C_{y2} + 4.d.cst & 0 & 0 & 0 & 0 & 0 & 0 & 0 \\
 0 & 0 & C_{s1} + C_{p1} & -C_{s1} & 0 & 0 & 0 & 0 & 0 \\
 0 & 0 & -C_{s1} & C_{p1} + C_{s1} + C_m.R_p^2 & -C_m.R_p.R_r & 0 & 0 & 0 & 0 \\
 0 & 0 & 0 & -C_m.R_p.R_r & C_{p2} + C_{s2} + C_m.R_r^2 & 0 & 0 & 0 & -C_{s2} \\
 0 & 0 & 0 & 0 & 0 & \frac{\mu h^2 N_0}{2r q_3} + d_r + 2dr^2(1 + \cos(\alpha)) & I_{D3}(\Omega + \dot{q}_3) & 0 & 0 \\
 0 & 0 & 0 & 0 & 0 & -(\Omega + q_3) I_{D3} - 2d(\mu r h + r^2 \sin(\alpha)) & d_r & 0 & 0 \\
 0 & 0 & 0 & 0 & -C_{s2} & 0 & 0 & 0 & C_{s2} + C_{p2}
 \end{bmatrix} \quad (34)$$

$[K(t)]$ is the stiffness matrix and written as:

$$[K(t)] = [K_e(t)] + [K_s] \quad (35)$$

where $[K_e(t)]$ is the linear time varying mesh stiffness matrix:

$$[K_e(t)] = (L_\delta)^T . L_\delta . k(t) \quad (36)$$

where L_δ is defined by:

$$\{q\} = \{y_1 \ y_2 \ \theta_M \ \theta_P \ \theta_R \ q_1 \ q_2 \ q_3\}$$

$[M]$ is a matrix composed of the terms of masses and inertias and is expressed by:

$$[M] = \text{diag}(m_{b1}, m_{b2}, I_M, I_P, I_R, I_{D1}, I_{D2}, I_{D3})$$

with m_{b1} and m_{b2} is the mass of blocks 1 and 2

$[C]$ is the damping matrix and is defined by:

$$L_\delta = [s_1 \ -s_1 \ 0 \ s_2 \ s_3 \ 0 \ 0 \ 0] \quad (37)$$

and R_p, R_r and β are defined in table 3.

$[K]$ is the stiffness matrix of the bearing and shafts and can be written by:

$$[K] = \begin{bmatrix} k_{y1} & 0 & 0 & 0 & 0 & 0 & 0 & 0 & 0 \\ 0 & k_{y2} + 4.k.cst & 0 & 0 & 0 & 0 & 0 & 0 & 0 \\ 0 & 0 & k_{s1} & -k_{s1} & 0 & 0 & 0 & 0 & 0 \\ 0 & 0 & -k_{s1} & k_{s1} & 0 & 0 & 0 & 0 & 0 \\ 0 & 0 & 0 & 0 & k_{s2} & 0 & 0 & 0 & -k_{s1} \\ 0 & 0 & 0 & 0 & 0 & 2N_0h + k_r + 2kr^2(1 + \cos(\alpha)) & \frac{\mu h^2 N_0}{2r} & 0 & 0 \\ 0 & 0 & 0 & 0 & 0 & -2\mu r N_0(1 + \cos(\alpha)) - 2kr(\mu h + r.\sin(\alpha)) & k_r + 2N_0(h + \mu^2 h + r.\mu.\sin(\alpha)) & 0 & 0 \\ 0 & 0 & 0 & 0 & -k_{s2} & 0 & 0 & 0 & k_{s2} \end{bmatrix}$$

The gear mesh stiffness remains constant in the case of a deformable tooth, or the assumption cannot be maintained and the introduction of the tooth deflection under load leads to having a variable stiffness engagement. The gear mechanism generates a torsional stiffness that changes with the angle of rotation which over time to introduce a more realistic engagement functions.

Indeed, as the number of pairs of teeth in contact is generally not constant during the engagement, the transmitted load is spread over these pairs of teeth. The variation of the stiffness of meshing can be approximated by a niche representation.

Fig. 13 shows this approximation plotted against time for helical gear mesh stiffness.

It is modeled by real profile (Walha et al., 2009), the maximum values of stiffness correspond to two pairs in contact and the minimum values correspond to one pair in contact.

The characteristics of the gear and pinion used in the numerical calculate were listed in Table 2. Using the means values presented in Tables 1 and 3, the Eigen frequencies of the system are presented and computed in Table 4.

Table3. The toothed wheels characteristics.

	Pinion	Toothed wheel
Number of teeth	20	40
Mass (kg)	0.6	2.5
Moment of inertia (kg/m ²)	2.6 10 ⁻⁴	4.510 ⁻⁴
Radius of the base circle (m)	0.025	0.055
Module (mm)	3	
Torsional damping bearings (N.m.s/rad)	C _{p1} =0.005 C _{p2} =0.005	
The average meshing damping (N.m.s/rad)	c _m =0.01	
Torsional stiffness of the shaft (N.m/rad)	k _{s1} = k _{s2} =10 ⁵	
Torsional damping of the shaft (N.m.s/rad)	C _{s1} = C _{s2} =0.005	
Helix angle (degré)	β=20°	
Pressure angle (degré)	α _g =20	
Tooth width (mm)	23	
Contact ratio	c=1.6	

Table 4. Eigen frequencies of the system.

Eigen frequencies (Hz)	f ₁	f ₂	f ₃	f ₄	f ₅	f ₆	f ₇	f ₈
	0	94	545	580	598	729	846	2078

Simulated angular velocity on motor in the input and disc brake in the output are represented by Fig. 14. Fig. 15 exhibits the time signal to the pinion angular velocity and Fig. 16 shows the time signal and the frequency spectrum corresponding to the pinion.

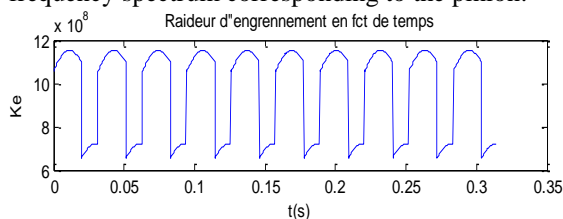


Fig.13. Helical Gear mesh stiffness modeling

The nonlinear motion equations are solved using an appropriate Runge Kutta algorithm in order to determine their dynamic behavior.

Simulated angular velocity on motor in the input and disc brake in the output are represented by Fig.14. Fig. 15 exhibits the time signal to the pinion angular velocity and Fig. 16 shows the time signal and the frequency spectrum corresponding to the pinion angular velocity.

The complexity of the dynamic study thanks to the large number of influencing parameters makes the analysis of a coupled system difficult. The gear mesh stiffness and the self-excited vibrations of the disc

brake model are two excitation sources. The main result is the increase of vibrations and this increase can be damage the transmission and in particular at

the level of teeth.

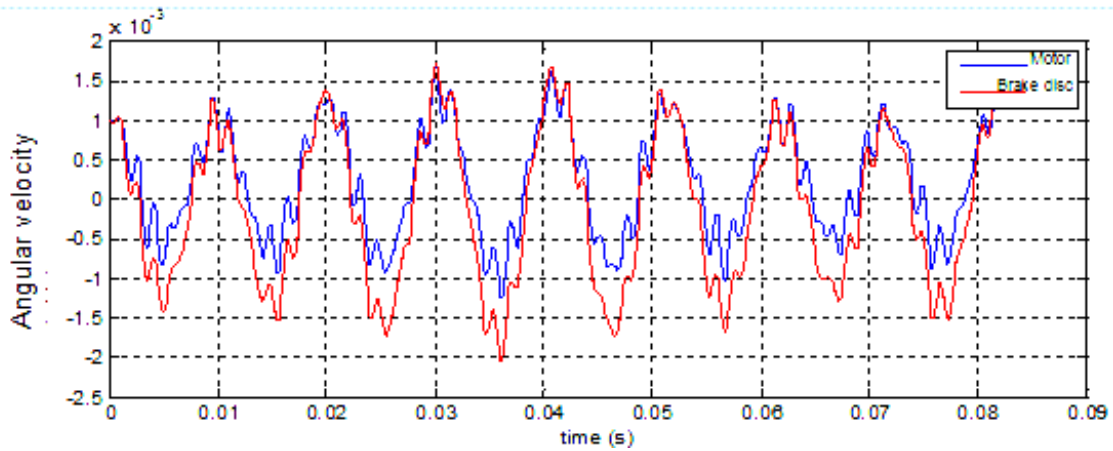


Fig.14. Time signal corresponding to the motor and brake disc angular velocity

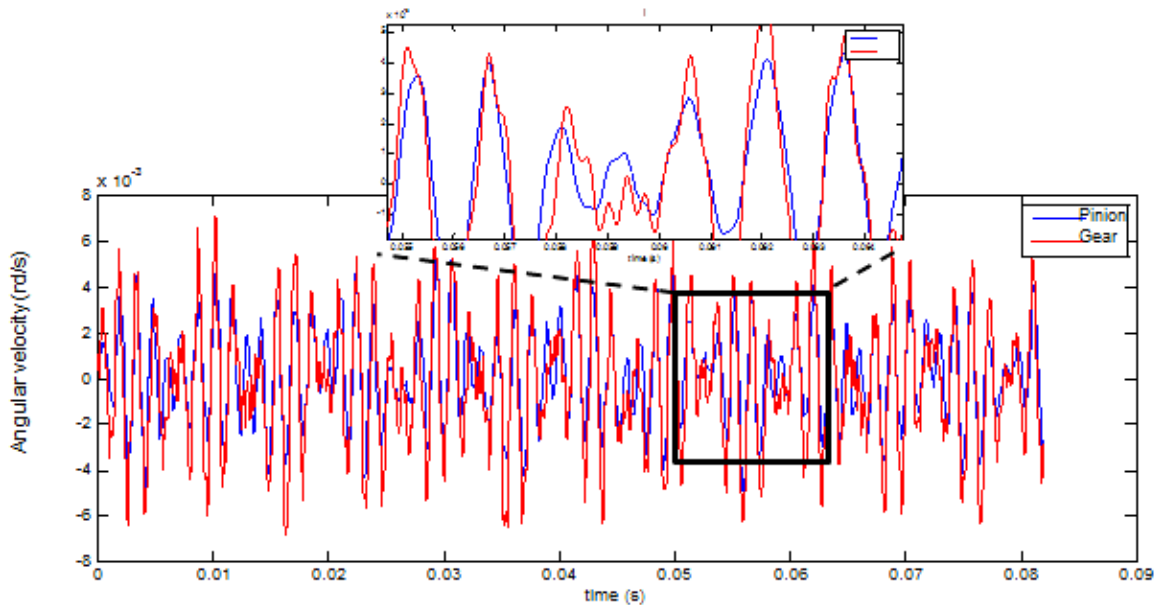


Fig. 15. Time signal corresponding to the two gear angular velocity

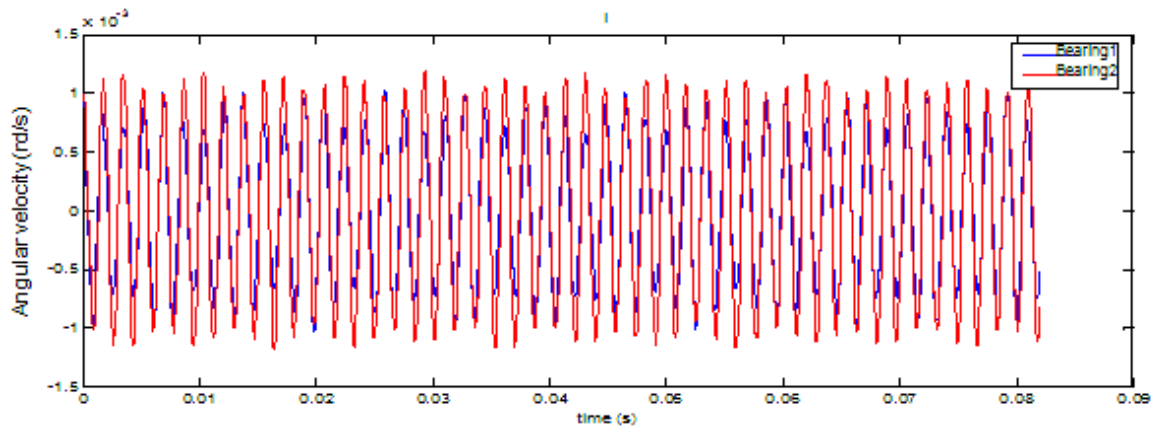


Fig. 16. Time signal corresponding to the two bearing angular velocity

CONCLUSIONS

In this present study, we have developed a new mathematical model with multi friction contacts, and to give a contribution on identifying the physical and geometrical parameters that can affect the Lyapunov stability of a disc brake system. This model takes account the self-excited vibrations; the main causes of squeal. The variations of input rotational speed, phase shift angle, coefficient of friction and the linear stiffness and damping is studied as well. Simulation results show the importance of playing on the characteristics of the components and form of brake pads.

In the second part, a nonlinear mechanical model with eight degrees of freedom is detailed in this paper to study the dynamic behavior of the disc brake coupled with helical gear. Amplification of the vibration is the most interesting results where we can see the influence of a braking system in the dynamic behavior of a single stage gear. The governing nonlinear time varying motion equation formulated is resolved by the analytic fifth-order Runge-Kutta method.

REFERENCES

- Andersson A., Vedmar L., A dynamic model to determine vibrations in involute helical gears, *J. Sound. Vib.*, Vol. 260, pp. 195–212(2003).
- Alexander, F., Drozdetskaya, O., and Waltersberger, B., " On the minimal model for the low frequency wobbling instability of friction discs." *Eur. J. Mech. A-Solid.*, Vol.30, No.5, pp.665-672(2011).
- Fosberry R.A.C. and Holubecki Z., "Disc brake squeal: its mechanism and suppression". *Technical report, Motor Industry Research Association , Warwickshire, England* (1961).
- Hagedorn, P., et al. "Self-Excited Vibrations and Damping in Circulatory Systems." *J. of App. Mech.*, Vol.81, No.10, pp.101009(2014).
- Hochlenert, D., Spelsberg-Korspeter, G., Hagedorn, P., "Friction induced vibrations in moving continua and their application to brake squeal", *ASME J. of App. Mech.*, Vol. 74, pp. 542–549(2007).
- Hochlenert, D., Spelsberg-Korspeter, G., & Hagedorn, P., "A note on safety-relevant vibrations induced by brake squeal", *J. Sound. Vib.*, Vol. 329, No. 19, pp. 3867–3872(2010).
- Hochlenert, D., "Nonlinear stability analysis of a disk brake model." *Non. Dyns.*, Vol. 58, No.1-2, pp. 63-73(2014).
- Jearsiripongkul, T., "Squeal in Floating Caliper Disk Brakes: A Mathematical Model". *Doctoral Thesis, Technische Universitat Darmstadt*, (2005).

- Khabou, M. T., Ksentini, O., Jarraya, A., Abbes, M. S., Chaari, F., Haddar, M., "Influence of disk brake friction on the dynamic behaviour of a directly coupled spur gear transmission". *Multidiscip. Model. Mater. Struct.*, Vol. 10, No. 2, pp. 146-162(2014).
- Kinkaid, O.M. O'Reilly, P. Papadopoulos, "Automotive disc brake squeal", *J. Sound. Vib.*, Vol.267, No.1, pp. 105–166(2003).
- Liu, P., Zheng, H., Cai, C., Wang, Y. Y., Lu, C., Ang, K. H., Liu, G. R., "Analysis of disc brake squeal using the complex eigenvalue method", *App. Acoustics.*, Vol. 68, No.6, pp. 603-615(2007).
- Oberst, S., and Lai, J. C. S., "Chaos in brake squeal noise *J. Sound. Vib.*, Vol. 330, No.5, pp. 955-975(2011).
- Ouyang, H., Mottershead, J.E., Brookfield, D.J., James, S., Cartmell, M.P., "A methodology for the determination of dynamic instabilities in a car disc brake", *Int. J. Veh. Des.*, Vol. 23, No.(3/4), pp. 241–262(2000).
- Shin, K., et al. "Analysis of disc brake noise using a two-degree-of-freedom model". *J. Sound. Vib.*, Vol. 254, No. 5, pp.837-848(2002).
- Spelsberg-Korspeter, G., Hochlenert, D., Kirillov, Hagedorn, O.N., "In-and out-of-plane vibrations of a rotating plate with frictional contact: investigations on squeal phenomena", *ASME J. of App. Mech.*, Vol.76, No.4, 041006-1–15(2009).
- Tuchinda, A., Hoffmann, N.P., Ewins D.J., Keiper W., "Effect of Pin Finite Width on Instability of Pin-On-Disc Systems", *Proceedings. IMAC.*, Vol. 1, pp. 552–557(2002).
- Tuchinda, A., Hoffmann, N. P., Ewins, D. J. and Keiper, W., "Mode Lock-in Characteristics and Instability Study of the Pin-On-Disc System", *Proceedings. IMAC.*, Vol. 1, pp. 71–77(2001).
- von Wagner, U., Hochlenert, D., Jearsiripongkul, T., Hagedorn, P., "Active control of brake squeal via Smart pads", *SAE Paper* No. 01-2773 (2004).
- von Wagner, U., Hochlenert, D., and Hagedorn, P. "Minimal models for disk brake squeal". *J. Sound. Vib.*, Vol. 302, No. 3, pp. 527-539(2007).
- Walha L., Driss Y., Fakhfakh T., "Effect of manufacturing defects on the dynamic behaviour for a helical two-stage gear system", *Mech & Ind.*, Vol. 10, pp. 365–376 (2009).
- Y. Denou, M. Nishiwaki, "First order analysis of low frequency disk brake squeal", *SAE paper*, No. 01-3136 (2001).

NOMENCLATURE

θ_M, θ_p and θ_R : The angular displacement of the motor, the pinion and the toothed wheel respectively;

q_1, q_2 and q_3 : Three cardan angles;
 y_1 and y_2 : The vertical displacement of the two shafts of transmission
 h : Thickness;
 k_r : Rotational stiffness;
 d_r : Rotational damping coefficient;
 I_D : The inertia tensor;
 I_{D1}, I_{D2} : Moment of inertia, with respect to \mathbf{d}_1 and \mathbf{d}_2 ;
 I_{D3} : Moment of inertia, with respect to \mathbf{d}_3 ;
 μ : friction coefficient
 $\mathbf{d}_i, \mathbf{n}_i, \mathbf{a}_i$ and \mathbf{b}_i ($i = 1, 2, 3$): Coordinate systems;
 α : Angle of phase shift;
 r : Radius of the disc;
 k : Nominal contact stiffness;
 d : Nominal contact damper;
 N_0 : Preload;
 $\omega_{N \rightarrow D}$: The resulting angular velocity;
 Ω : Constant speed of rotation;
 $\mathbf{P}_1, \mathbf{P}_2, \mathbf{P}_3$ and \mathbf{P}_4 : The vectors of contact points;
 h_1, h_2, h_3 and h_4 : The corresponding movements of the pads;
 $\mathbf{F}_1, \mathbf{F}_2, \mathbf{F}_3$ and \mathbf{F}_4 : The resulting contact forces on the disc;
 M : The resisting torque on the disc;
 M_A : The constraint torque;
 Ω_{crit} : Critical speed;
 $[M]$: Mass matrix;
 $[C]$: Damping matrix;
 $[K(t)]$: Stiffness matrix;
 s_1, s_2 and s_3 : The coefficients of $K(t)$;
 $[K_e(t)]$: The linear time varying mesh stiffness matrix;
 C_{p1}, C_{p2} : Torsional damping bearings;
 c_m : the average meshing damping;
 k_{s1}, k_{s2} : Torsional stiffness of the shaft;
 k_{y1}, k_{y2} : Stiffness of the bearing;
 C_{s1}, C_{s2} : Torsional damping of the shaft;
 β : Helix angle;
 α_g : Pressure angle ;
 $f(i=1..8)$: Eigen frequencies.